REPORT SNO. 7633-2021

Norwegian University of Life Sciences

Hydropower: gas supersaturation and the role of aquatic plant photosynthesis for fish health

River Otra. Photo: Benoît Demars (NIVA)

Norwegian Institute for Water Research

REPORT

Main Office
Gaustadalléen 21
NO-0349 Oslo, Norway
Phone (47) 22 18 51 00

NIVA Region South
Jon Lilletuns vei 3
NO-4879 Grimstad, Norway
Phone (47) 22 18 51 00

NIVA Region East
Sandvikaveien 59
NO-2312 Ottestad, Norway
Phone (47) 22 18 51 00

NIVA Region West
Thormøhlensgate 53 D
NO-5006 Bergen Norway
Phone (47) 22 18 51 00

NIVA Denmark
Njalsgade 76, 4th floor
DK 2300 Copenhagen S, Denmark
Phone (45) 39 17 97 33

Internet: www.niva.no

Title	Serial number	Date
Hydropower: gas supersaturation and the role of aquatic plant photosynthesis for fish health	7633-2021	10.02.2021
Author(s) Benoît O.L. Demars, Peter Dörsch, Kirstine Thiemer, François Clayer, Susanne C. Schneider, Sebastian F. Stranzl, Ulrich Pulg, Gaute Velle	Topic group Fresh water biology	Distribution Open
	Geographical area Agder	Pages 23 + appendix

Client(s)	Client's reference
Krypsivprosjektet på Sørlandet (KPS). Sekretariat: Fylkesmannen i Agder, Miljøvernavdelingen	Anna Asgard
	Printed NIVA
	Project number 190151

Summary

Fish and invertebrates breathing in water supersaturated with gas (total dissolved gas; TDG), e.g. at the outlet of hydropower plants, may develop gas bubble disease (analogous to the bends in humans). Aquatic plants also influence the gas saturation, and here we quantified to what extent the mass development of an aquatic plant (*Juncus bulbosus*) downstream Brokke hydropower plant in southern Norway could increase TDG and the risk for aquatic animal health.

We found that *J. bulbosus* mass development could account for up to 5 % extra TDG supersaturation through photosynthesis, that is 105 % TDG saturation on its own. We can expect chronic health issues and acute mortality for fish and invertebrates if the added gas saturation causes the TDG supersaturation to increase to levels above a species' tolerance, which is 110 % for acute mortality of Atlantic salmon (*Salmo salar*) in surface waters. Since TDG is reduced by about 10 % per meter water depth, fish may escape harmful supersaturation by moving deeper. However, the photosynthesis peak in gas saturation corresponds to surface feeding time of salmonids, so further studies in fish behaviour are required.

Four keywords	Fire emneord
1. Gas supersaturation	1. Gassovermetning
2. Fish	2. Fisk
3. Aquatic plants	3. Vannplanter
4. Photosynthesis	4. Fotosyntese

This report is quality assured in accordance with NIVA's quality system and approved by:

Benoît O.L. Demars	*Therese Fosholt Moe*	*Therese Fosholt Moe*
Project Manager	Quality Assurance	Research Manager

ISBN 978-82-577-7369-4
NIVA-report ISSN 1894-7948

Hydropower: gas supersaturation and the role of aquatic plant photosynthesis for fish health

Preface

All authors were involved in discussions to design the study. Sebastian Stranzl and Benoît Demars were responsible for deploying sensors and reporting results. Kirstine Thiemer, François Clayer, Susanne Schneider and Benoît Demars collected and prepared the water samples for gas chromatography. Peter Dörsch analysed the samples by gas chromatography. Benoît Demars ran the calculations and drafted the report together with Gaute Velle. Most authors participated in a workshop to discuss the results and commented on the report.

This project has been funded by Krypsivprosjektet på Sørlandet (KPS). Kristin Uleberg and Anna Asgard administrated the project for KPS.

Oslo, 09.02.2021

Benoît O.L. Demars

Table of contents

1 Introduction 8
1.1 Background 8
1.2 The need to invoke a noble gas 9
1.3 CO_2 as a potential limiting factor for photosynthesis 9
1.4 Research questions 10

2 Methods 11
2.1 Study area and sampling stations 11
2.2 Equipment 11
2.3 Collection of water samples and gas analyses 13
2.4 Quantification to total dissolved gas saturation from individual gases 13
2.5 Enhanced photosynthesis caused by supersaturation 13

3 Results and discussion 14
3.1 Dissolved gas observed in the field 14
3.2 Diel change in dissolved oxygen 18
3.3 Role of photosynthesis for gas supersaturation 18

4 Conclusion 21

5 References 22

Appendix A 24
Appendix B 25
Appendix C 28

Abstract

Fish and invertebrates breathing in water supersaturated with total dissolved gas (TDG) at the outlet of hydropower plants may develop gas bubble disease (analogous to the bends in humans), with acute mortality from about 110 % TDG in Atlantic salmon (*Salmo salar*). Aquatic plants also influence the gas saturation, and here we quantified to what extent the mass development of an aquatic plant (*Juncus bulbosus*) downstream Brokke hydropower plant in southern Norway could increase TDG and the potential risk for aquatic animal health.

We first explained the principles of photosynthesis and gas exchange to show how TDG may be generated by aquatic photosynthesis. We separated the oxygen supersaturation caused by aquatic plants from the physical supersaturation caused by the hydropower plant with the ratio of oxygen to noble gas argon. We used sensors (TDG, oxygen, CO_2) and gas chromatography (N_2, O_2, Ar, CO_2, CH_4, N_2O) to estimate TDG and allow the partitioning of physical from biological processes. We further explored, using field and published laboratory data, to what extent CO_2 supersaturation from the hydropower plant could increase the rate of photosynthesis of aquatic plants and lead to even higher TDG supersaturation.

We found that *J. bulbosus* mass development could account for up to 5 % extra TDG supersaturation through photosynthesis, that is 105 % TDG saturation on its own, in late afternoon and evening. We can expect chronic health issues and acute mortality for fish and macroinvertebrates if the added gas saturation causes the TDG supersaturation to increase to levels above a species' tolerance, which is 110 % for acute mortality of Atlantic salmon in surface waters. Since TDG is reduced by about 10 % per meter water depth, fish may escape harmful supersaturation by moving deeper. The timing of the photosynthesis peak corresponds, however, to the timing of surface feeding by salmonids (personal observations), thus further research is needed to link individual fish behaviour to total gas supersaturation and the role of photosynthesis.

Utvidet norsk sammendrag

Tittel: Vannkraft: Gassovermetning og effekter av vannplanters fotosyntese på fiskehelse
År: 2020
Forfatter(e): Benoît O.L. Demars, Peter Dörsch, Kirstine Thiemer, François Clayer, Susanne C. Schneider, Sebastian F. Stranzl, Ulrich Pulg, Gaute Velle
Utgiver: Norsk Institutt for Vannforskning, ISBN 978-82-577-7369-4

Elvevann har som regel ca 100 % metning av gass (det vil si luft) ved vannoverflaten. Betydelig gassovermetning, det vil si mye mer enn 100 % metning av luft, kan forekomme under flomepisoder eller nedstrøms fossefall i dype kulper (opptil 115 %), når ekstra luft «presses» inn i vannet. Gassovermetning kan også oppstå i vannkraftverk når luft suges inn i tunnelsystemet (over 200 % observert fra Brokke kraftverk i Otra, Agder). Fordi det også er høyt trykk i tunnelsystemet løses luften opp i vannet, mens gassovermetningen oppstår først når trykket reduseres etter at vannet har passert turbinen. Luften er da blitt som bittesmå bobler i vannet. Ved slik gassovermetning risikerer fisk og bunndyr å bli rammet av gassblæresyke, tilsvarende dykkersyke hos mennesker. Lakseyngel og enkelte arter bunndyr dør fra ca 110 %, mens effekter hos de fleste andre organismer foreløpig er ukjente.

Vannplanter og alger kan også påvirke gassmetningen, ettersom disse gjennom fotosyntesen tar opp karbondioksid (CO_2) og produserer oksygen. Denne oksygenproduksjonen kan øke mengden oksygen i vannet, og dermed føre til økt gassovermetning. Hvor stor denne økningen blir vil være avhengig av lysintensitet og hvor mye vannplanter det er (biomasse). Dette betyr at tett krypsivvekst kan føre til økt gassovermetning, noe som igjen vil føre til økt risiko for skade på akvatiske organismer. Sammenhengen mellom gassovermetning og krypsiv er likevel foreløpig dårlig kjent, og det er dette som er undersøkt i denne rapporten.

Kraftverket ved Brokke i Otra produserer periodevis høy gassovermetning. Samtidig er det tett krypsivvekst i Rysstadbassenget nedstrøms Brokke. I dette området varierer gassovermetningen ofte gjennom døgnet, noe som både kan skyldes endringer i vannføring og endringer i fotosyntese. I dette arbeidet har vi undersøkt om krypsiv nedstrøms Brokke bidrar til økt gassovermetning, og i så fall hvor mye. Dette er gjort ved å bruke gassen argon som referanse. Argon og oksygen har lik løselighet i vann, men mens mengden argon i vann kun er avhengig av fysiske prosesser, vil mengden oksygen være avhengig av både fysiske og biologiske prosesser. Det er dermed mulig å bruke forholdet mellom argon og oksygen for å skille mellom gassovermetning som er forårsaket av biologiske prosesser, det vil si fotosyntese, og mengden som er forårsaket av fysiske prosesser, det vil si kraftverket ved Brokke. Som et tilleggsmoment har vi undersøkt om gassovermetning kan føre til økt plantevekst. Dette kan skje fordi plantene bruker CO_2 i fotosyntese, og mengden CO_2 øker ved høyere gassovermetning fra kraftverket. Dersom CO_2 er en begrensende faktor for fotosyntese, vil økt konsentrasjon av CO_2 som følge av gassovermetningen bidra til økt fotosyntese.

For å undersøke sammenhengen mellom gassovermetning og krypsiv undersøkte vi ni lokaliteter i Otra, fra utløpet av Brokke til ca 11 km nedstrøms Brokke (**Figur 3**). Fra syv av disse stasjonene ble det tatt vannprøver hver andre time gjennom ett døgn, og gassammensetningen i prøvene ble senere analysert i laboratoriet ved hjelp av gasskromatografi. Vi registrerte også vannføring, gassovermetning og lysintensitet ved et utvalg stasjoner (**Tabell 1**). For å finne ut hvorvidt gassovermetning fra kraftverket fører til økt fotosyntese brukte vi konsentrasjonen av CO_2 og O_2, supplert med informasjon fra litteraturen.

Målingene viste at det i prøvetakingsperioden var høyest gassovermetning ved midtre og nedre del av Rysstadbassenget. Her var det også 15 % variasjon i gassovermetning gjennom døgnet. Variasjonen skyldes endringer i både vannføring, utgangsmetning fra Brokke og fotosyntese. Forholdet mellom oksygen og argon indikerer at oksygenproduksjonen fra krypsiv bidrar til å øke gassovermetningen opptil 5 %. Av dette vil ca en femtedel være forårsaket av økt tilgjengelighet av CO_2 i vannet som følge av at gassovermetning øker fotosyntesen.

Økningen i gassovermetning som er forårsaket av fotosyntese hos krypsiv kan bidra til bobledannelse og forhøyet dødelighet og skader på fisk og bunndyr. Skadene vil være mest betydelige dersom økningen fører til at gassovermetningen overstiger ca 110 %, men fisk tåler O_2-overmetning bedre enn N_2-overmetning. Siden TDG reduseres med ca. 10 % per meters vanndybde, kan fisk unnslippe skadelig gassovermetning ved å bevege seg dypere. Men tidspunktet for oksygenmetningstopp (ettermiddag-kveld) tilsvarer tidspunktet for overflatefôring hos salmonider (personlige observasjoner). Det er derfor behov for videre forskning som knytter individuell fiskeatferd til total gassovermetning og fotosyntesens rolle.

1 Introduction

1.1 Background

Total dissolved gas (TDG) supersaturation (i.e. > 100 % total dissolved gas, mostly N_2 and O_2) is an overlooked hazard to aquatic life in rivers downstream of hydroelectric power plants. TDG supersaturating occurs downstream of hydroelectric power plants when air is dissolved in water under high pressure in the tunnel system, and the pressure decreases at the plant outlet in the river (Weitkamp & Katz, 1980). Aeration of TDG may occur slowly and over several km before dissolved gas saturation return to normal. Organisms that respire in water develop gas bubbles in tissues because of surplus gas, which may have adverse effects, such as gas bubble disease (analogous to the bends in humans) in fish and invertebrates (see Stenberg *et al.*, 2020; Pulg *et al.*, 2016a; Pulg *et al.*, 2016b; Velle *et al.*, 2017). Acute mortality induced by TDG supersaturation commences from about 110 % TDG in Atlantic salmon (*Salmo salar*) (Stenberg *et al.*, 2020).

In the River Otra, TDG supersaturation reached up to 200 % at the outlet of the Brokke hydropower plant and supersaturation was detected 30 km downstream (Pulg *et al.*, 2016a; Pulg *et al.*, 2016b, unpublished data). Consequently, about 4 km of the River Otra downstream of the outlet has no fish and a low density and diversity of macroinvertebrates, in an area expected to be highly productive (Pulg *et al.*, 2018). Fish can avoid supersaturation by moving to deeper water because more gas can dissolve in water at greater pressures. TDG is reduced by about 10 % per meter water depth. Rainbow trout (*Oncorhynchus mykiss*) has been shown to actively avoid supersaturated water by swimming deeper (Johnson *et al.*, 2010), however, we do not know to what extent European freshwater species respond to TDG supersaturation.

Aquatic plant photosynthesis is known to generate large diel changes in O_2 in water, particularly in systems with low reaeration rate (i.e. low gas exchange rate between water and air) and high plant biomass (e.g. Sculthorpe, 1967). Since dissolved oxygen represents 34 % of total dissolved gases in water (**Fig. 1**), diel changes in O_2 due to photosynthesis could make supersaturation worse for fish, particularly around midday. Large diel changes have been observed before in the River Otra at the downstream end of Rysstad basin (Straume) holding large standing biomass of *Juncus bulbosus*. The observed diel changes in total dissolved gases were about 10 % (Pulg *et al.*, 2016a), but it is not known whether this is due to changes in discharge and degree of supersaturation from the power plant or possibly photosynthesis.

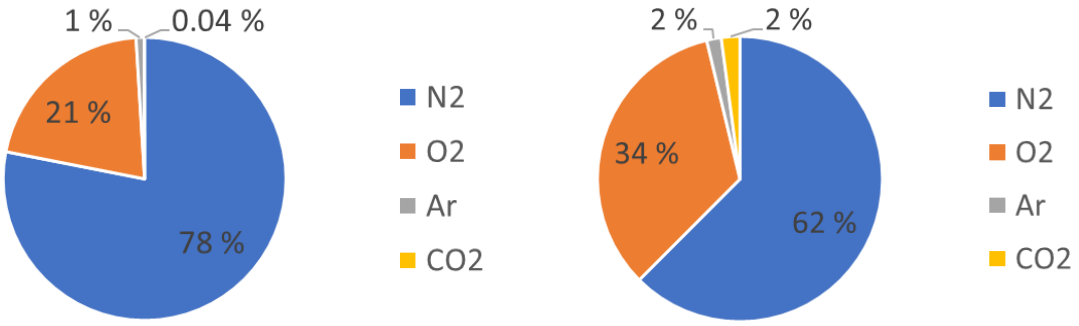

Fig. 1. Proportion of gases in dry air (left) and in water at 10°C (right).

1.2 The need to invoke a noble gas

Argon is a noble gas which does not interact chemically in the environment. Hence, argon gas saturation in the river will only be dependent on physical processes. Argon has similar diffusivity and solubility in water as oxygen. Thus, it is possible to use argon to separate the contribution of physical processes from biological processes in oxygen gas saturation, i.e. separate the role of the hydropower plant from *J. bulbosus* photosynthesis (Craig & Hayward, 1987).

In a closed system, photosynthesis should not alter total dissolved gas saturation, as CO_2 is consumed to produce O_2. Indeed, we have (in the presence of light):

$$6CO_2 + 6H_2O \rightarrow C_6H_{12}O_6 + 6O_2$$

Thus, for 6 moles of CO_2 uptake by primary producers (e.g. *J. bulbosus*), 6 moles of O_2 are produced. In addition, 6 moles of water (H_2O) are consumed, and one mole of sugar ($C_6H_{12}O_6$) is produced, though this is not relevant for the gas balance.

Text Box 1.

Although CO_2 is 32 times more soluble in water than O_2, the partial pressure of CO_2 in the atmosphere is 523 times smaller than O_2 (20.95 % versus 0.04 % in dry air, **Fig. 1**). Thus, there is 16 times more dissolved O_2 than dissolved CO_2 in water at equilibrium with the atmosphere (**Fig. 1**). The flux *F* of gases (g gas m^{-2} s^{-1}) between the water and the atmosphere is:

$$F = kz(C_{SAT} - C)$$

where k is the gas exchange coefficient (s^{-1}), z depth (m), kz gas transfer velocity (m s^{-1}), C_{SAT} saturated concentration of gas (g m^{-3}), and C observed concentration of gas (g m^{-3}). The gas exchange coefficient is similar for O_2 and CO_2 with $k_{CO2} = 0.81\ k_{O2}$. The saturation deficit (or supersaturation) will be 16 times larger for CO_2 than O_2 for a given photosynthetic rate, that is the flux of CO_2 between the water and the atmosphere will be 0.81×16=13 times faster for CO_2 than O_2.

Moreover, CO_2 may also enter the carbonate equilibrium (depending on pH), notably in rivers with poor gas exchange rate (deep slow flowing rivers). The rate of formation of HCO_3 could be calculated following Stumm and Morgan (1981) from pH and HCO_3 concentrations (should these data be available) and kinetic constants of the equilibrium:

$$CO_2 + H_2O \leftrightarrow H^+ + HCO_3^-$$

Under high pH (abundant OH^-), the conversion of CO_2 to HCO_3 by hydroxylation would also be important to consider (Emerson, 1975), but this is not the case in Otra, as evidenced by NIVA long term pH data one kilometre downstream Brokke.

In an open system (e.g. river), gas exchange rates between the water and the atmosphere depend on the solubility, diffusivity and saturation deficit (differences in gas partial pressures between the water and the atmosphere) of gases. CO_2 behaves differently to O_2 and this lead to total gas oversaturation (see **Text Box 1**).

The take home message is that since dissolved O_2 stay a longer time in water than dissolved CO_2, dissolved oxygen produced by photosynthesis may contribute to total dissolved gas supersaturation.

1.3 CO_2 as a potential limiting factor for photosynthesis

When CO_2 is a limiting factor, the increase in CO_2 due to gas supersaturation could increase the growth rate (photosynthesis) of *J. bulbosus*. This could in turn affect total gas supersaturation, with increased O_2 production, that may affect fish negatively. Liming has caused mass development of *J. bulbosus* in lakes, by increasing the rate of decomposition of sediment organic matter, boosting CO_2 and nutrient (N, P) supply for aquatic plant growth (Roelofs, Brandrud & Smolders, 1994). Laboratory short term additions of CO_2, under high light and sufficient nutrient availability (N, P), are known to boost aquatic plant photosynthesis (Blackmann & Smith, 1911), including *J. bulbosus* (Roelofs, Schuurkes & Smits, 1984; Sand-Jensen, 1987, **Fig. 2**). One lake experiment in Sweden reported an

increase *in J. bulbosus* growth rate when CO_2 was added (×10) to the water column in a lake with highly organic sediment and background CO_2 concentration around 50 µmol L^{-1} (Svedang, 1992). This means that CO_2 could be limiting *J. bulbosus* photosynthesis.

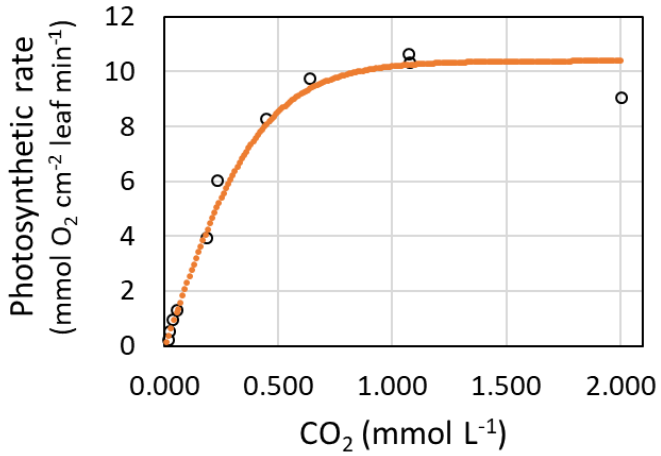

Text Box 2.
Fitted model is:

$$P = P_m \, tanh\left(\frac{\alpha CO_2}{P_m}\right) + R_0$$

with P photosynthetic rate, P_m CO_2 saturated photosynthetic rate, α CO_2 harvesting and photosynthetic energy conversion efficiency (the slope of the curve near the origin), R_0 rate of photosynthesis in the absence of CO_2.

Fig. 2. Photosynthetic rate of *Juncus bulbosus* (shoot with roots in water) as a function of dissolved CO_2 concentration (Sand-Jensen, 1987). See details in **Text Box 2**.

1.4 Research questions

Based on the need to find how gas supersaturation and outgrowth of *J. bulbosus* are mutually dependent, and based on the background information on argon and CO_2 given above, we ask the following research questions:

1. To what extent does O_2 produced by aquatic plants during photosynthesis increase the TDG supersaturation downstream of the Brokke hydropower plant, which in turn may cause harmful effects on fish?
2. To what extent does CO_2 supersaturation cause increased photosynthesis of aquatic plants, which in turn may cause increased levels of supersaturation and harmful effects on fish?

2 Methods

2.1 Study area and sampling stations

Sensors and sample collection were performed at nine sampling stations (**Table 1**, **Fig. 3**). Water samples were collected every two hours over 24 hours at seven stations and analysed at NMBU for six gases (**Table 1**, **Fig. 3**). NORCE monitored total dissolved gas saturation and dissolved oxygen at four stations, and CO_2 at one station, using sensors logging every 30 minutes. NIVA installed an additional four O_2 sensors and one atmospheric sensor and light (photosynthetic active radiation), using sensors logging at 15- minute intervals, deployed as part of the JPI Water Madmacs project.

This design allowed to test for changes in dissolved gas composition along a 10780 m long river section, divided in three parts: **Brokke to Rysstad** (3130 m, upper section), **Rysstad to Straume** (4660 m, middle section) and **Straume to Hekni** (2990 m, lower section). We expected the Rysstad basin (middle section) to generate the largest diel change in O_2, unrelated to the Brokke power plant outflow, because of the mass development of *J. bulbosus* in the Rysstad basin and previous results on total dissolved gases (Pulg *et al.*, 2016a).

2.2 Equipment

NORCE monitored total dissolved gas (TDG) with a Total Gas Analyzer 3.0 (Fisch- und. Wassertechnik; Pulg *et al.*, 2016a), based on the Weiss-saturometer principle (Weiss, 1970). The Total Gas Analyzer measures TDG pressure in a submerged gas permeable silicon hose connected to an underwater pressure sensor and an atmospheric pressure sensor above the surface water. The saturation is measured as the percent dissolved air in the water relative to expectation from ambient air pressure. The saturometer has an accuracy of ± 10 hPa, which is approximately ± 1 % TDG.

Table 1. Field sites (see **Fig. 3**). TDG=Total dissolved gas, atm=atmospheric pressure, light=photosynthetic active radiations

	EU89 coordinate system		NORCE	NMBU	NIVA
Station	Northing	Easting	Sensors	Hand samples	Sensors
Brokke power plant outflow	59.1194728	7.5133881	TDG, O_2	N_2, O_2, CO_2, Ar, CH_4, N_2O	
Brokke Otra upstream outflow	59.1194868	7.5137090		N_2, O_2, CO_2, Ar, CH_4, N_2O	
Rysstad Terskel	59.0976410	7.5281230	TDG, O_2, CO_2	N_2, O_2, CO_2, Ar, CH_4, N_2O	
Rysstad Øy	59.0993823	7.5280356	TDG, O_2	N_2, O_2, CO_2, Ar, CH_4, N_2O	O_2
Rysstad middle right	59.0889697	7.5484687			O_2
Rysstad middle left	59.0901028	7.5507781			O_2
Straume right	59.0674961	7.5728807		N_2, O_2, CO_2, Ar, CH_4, N_2O	O_2, light, atm
Straume left	59.0678875	7.5733180		N_2, O_2, CO_2, Ar, CH_4, N_2O	
Hekni	59.0427110	7.5654185	TDG, O_2	N_2, O_2, CO_2, Ar, CH_4, N_2O	

NIVA deployed three oxygen / temperature sensors in Rysstad (miniDOT, PME, Canada). At Straume, NIVA installed a monitoring station logging dissolved oxygen and water temperature (Xylem-Andeeraa optode 4831), photosynthetic active radiation (LICOR, Quantum LI190R-L), air temperature and atmospheric pressure (Barometer RM Young 061302V) using a Campbell datalogger (CR1000X). The monitoring station also has a modem (Campbell Scientific 4G modem CELL215) allowing to transfer data daily to Oslo headquarters. The monitoring station was later installed more permanently for one year, starting 25 November 2019, as part of JPI Water Madmacs project.

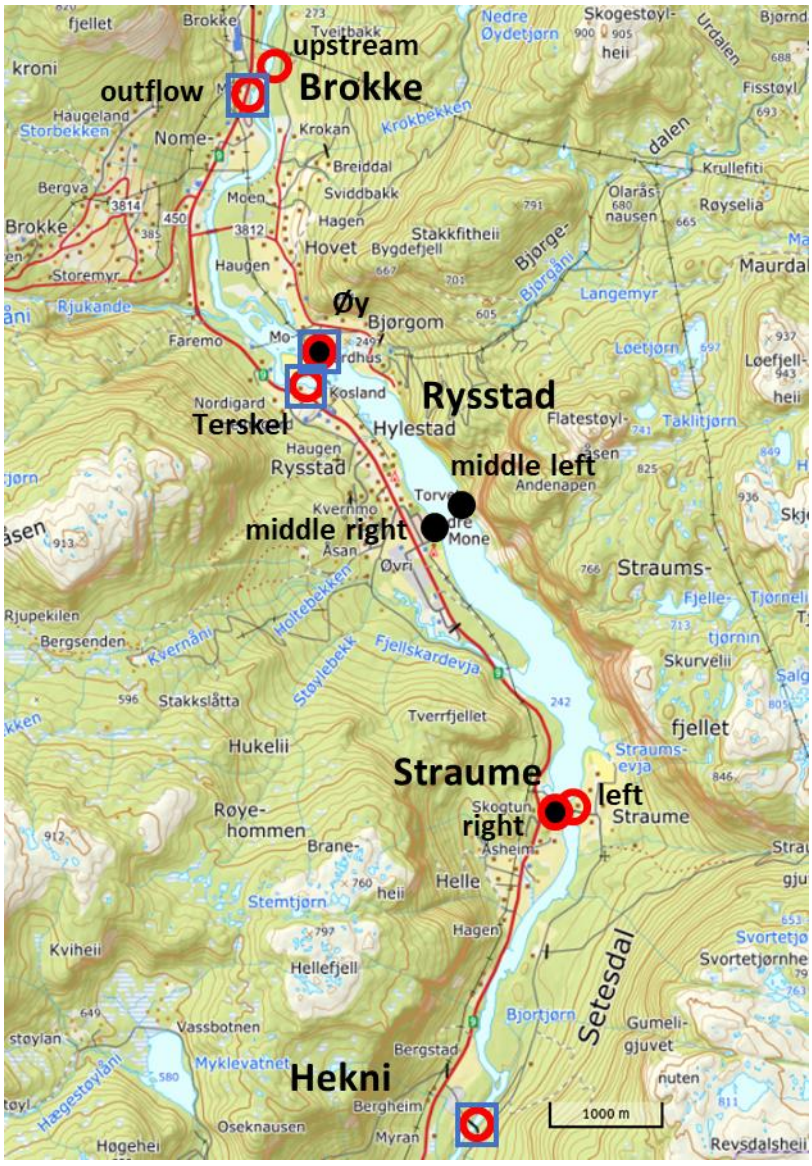

Fig. 3. Field sites: NORCE sensors (blue square), NMBU hand samples (red circle), NIVA sensors (black filled circle). See also **Table 1**. Map from Norgeskart.

2.3 Collection of water samples and gas analyses

Samples were collected by hand every two hours starting 12:00 on 4th August and ending 12:00 on 5th August. The water samples were collected in 120 mL glass bottles. Water bottles were filled to the rim and capped underwater, then crimped. Mercuric chloride was added to stop biological processes (100µL of half saturated solution per 120 mL bottle). The samples were kept cool (+4°C) and in the dark until the day of gas analysis. The samples were warmed and weighed at room temperature, a 30 mL helium headspace was created, the samples were weighed again (to determine the volume of water removed from the bottle), and shaken gently horizontally for at least an hour, prior to gas analysis of the headspace (**Appendix A: Fig. S1, S2**). Gas chromatography followed Yang *et al.* (2015).

2.4 Quantification to total dissolved gas saturation from individual gases

The results from gas chromatography give the concentration of dissolved gases (in ppm) in the headspace in equilibrium with the water. The concentration of dissolved gases in the water at equilibrium with the headspace can be calculated from the solubility of gases in water using Carroll, Slupsky and Mather (1991) for CO_2, Weiss and Price (1980) for N_2O, Yamamoto, Alcauskas and Crozier (1976) for CH_4, Millero, Huang and Laferiere (2002) for O_2, Hamme and Emerson (2004) for Ar and N_2. The quantities of gases in the headspace and water were summed to find the concentrations and partial pressures of dissolved gases from the water collected in the field. The proportion of individual gases in dissolved air were calculated from their individual molar concentration relative to the sum of molar concentrations of all six gases (**Fig. 1**). The observed partial pressure related to expected partial pressure (under field temperature and absolute atmospheric pressure) gave the excess partial pressure (saturation) of individual gases and samples. The total gas saturation was calculated from summing the products of individual gas saturation × proportion of gas in dissolved air (weighted average).

2.5 Enhanced photosynthesis caused by supersaturation

The extent to which CO_2 in supersaturation causes increased photosynthesis could only be answered by quantifying photosynthesis in the field under different CO_2 supersaturation conditions. Since we only monitored CO_2 over the course of one day under relatively low supersaturation conditions, we have to rely on quantitative assumptions based on the literature and available field data.

A preliminary study in southern Norway (Brokke, Laudal and Håverstad) suggested a 28 % increase in CO_2 concentration in the water downstream hydroelectric power plants (Moe & Demars, 2017). This could simply be due to cooler temperature, water supply from bottom of water reservoir, or overall TDG supersaturation produced by the power plant. The observed CO_2 concentrations in the water column were generally low (on average, 43 µmol L^{-1} upstream and 54 µmol L^{-1} downstream hydropower plant effluent), compared to the saturation rate of photosynthesis in *J. bulbosus* observed in lab experiments (about 500 µMol L^{-1}, Sand-Jensen, 1987; Roelofs, Schuurkes & Smits, 1984, **Fig. 2**). The small increase in CO_2 concentration could lead to a similar increase (+28 %) in *J. bulbosus* photosynthetic rate from 0.94 to 1.20 mMol O_2 cm^{-2} leaf min^{-1} (derived from Sand-Jensen, 1987, **Fig. 2**). This rate of increase is however unlikely in the field due to self-shading, i.e. light limitation (Binzer, Sand-Jensen & Middelboe, 2006).

3 Results and discussion

3.1 Dissolved gas observed in the field

First, we wanted to test whether there was a difference in the measured gas concentrations between the two different methods, i.e. sensors in the field and gas chromatography in the lab. Comparisons of dissolved gas concentration and TDG between sensors and gas chromatography are illustrated for Brokke, Hekni and Rysstad (Terskel and Øy) – in **Fig. 4-6**. Overall, determination by gas chromatography for oxygen and total dissolved gases was higher than recorded by the calibrated sensors. Discrepancies may be due to sample storage conditions (use of $HgCl_2$ to preserve samples for gas chromatography, unpublished results) rather than analytical method uncertainties (Fickeisen, Schneider & Montgomery, 1975) or sampling differences (surface water *versus* mid water column). The O_2:Ar ratio should not be affected much by these discrepancies, however. The CO_2 concentrations were relatively similar between the sensor deployed at Rysstad (Terskel) and determination by gas chromatography (**Fig. 6**). For the other relevant parameters measured, see **Text Box 3**.

Text Box 3.
Exact time of sampling (hh:mm), water temperature (°C), absolute atmospheric pressure (mbar) and photosynthetic active radiation (PAR, µmol quanta m^{-2} s^{-1}) were recorded in **Appendix B**. The concentrations of six dissolved gases (N_2O, CO_2, O_2, N_2, Ar, CH_4) by gas chromatography at the seven sites over a diel cycle were recorded in **Appendix C**. The sum of the six dissolved gases (TDG) was also recorded in **Appendix C**.

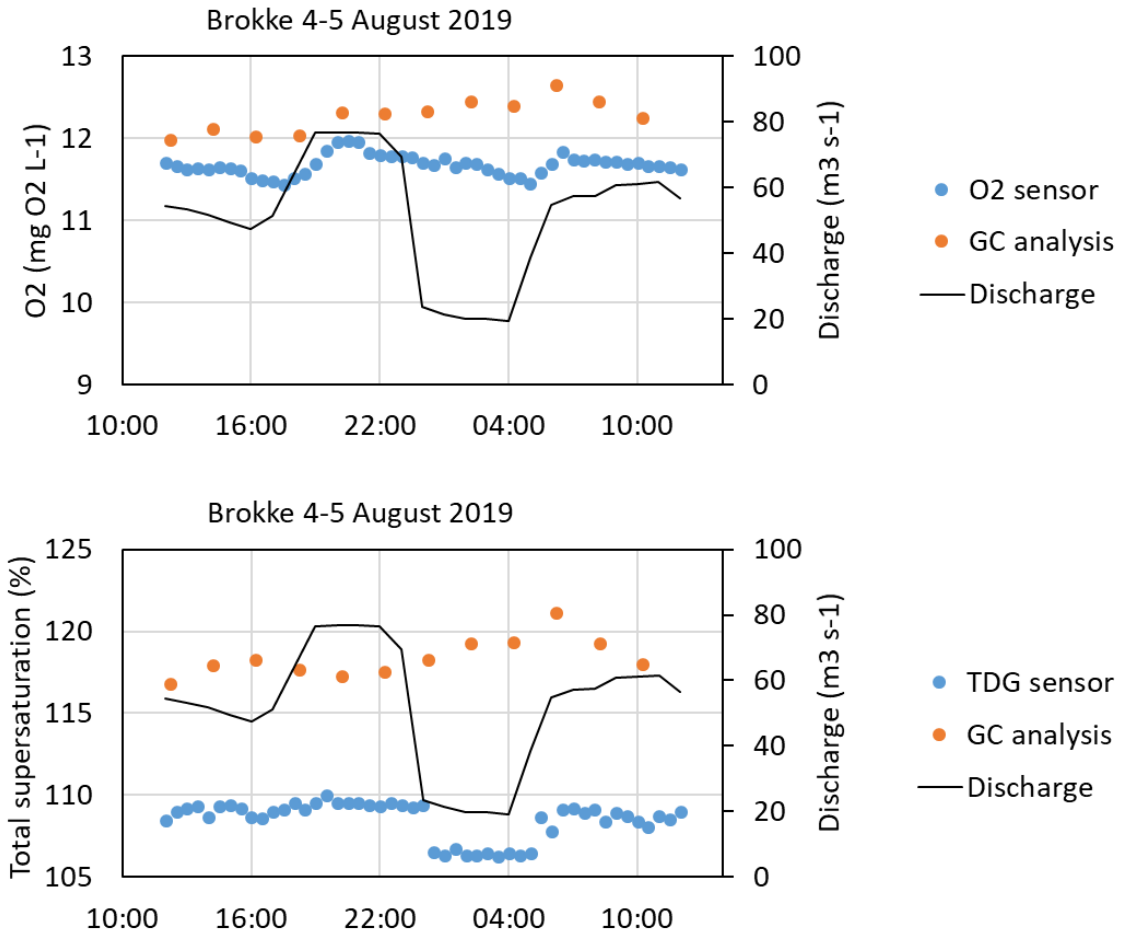

Fig. 4. Most upstream site, at outlet from Brokke: Brokke oxygen concentration (upper panel) and total dissolved gas supersaturation (TDG, lower panel). Comparison of data between sensors and determination by gas chromatography (GC). Discharge at Brokke.

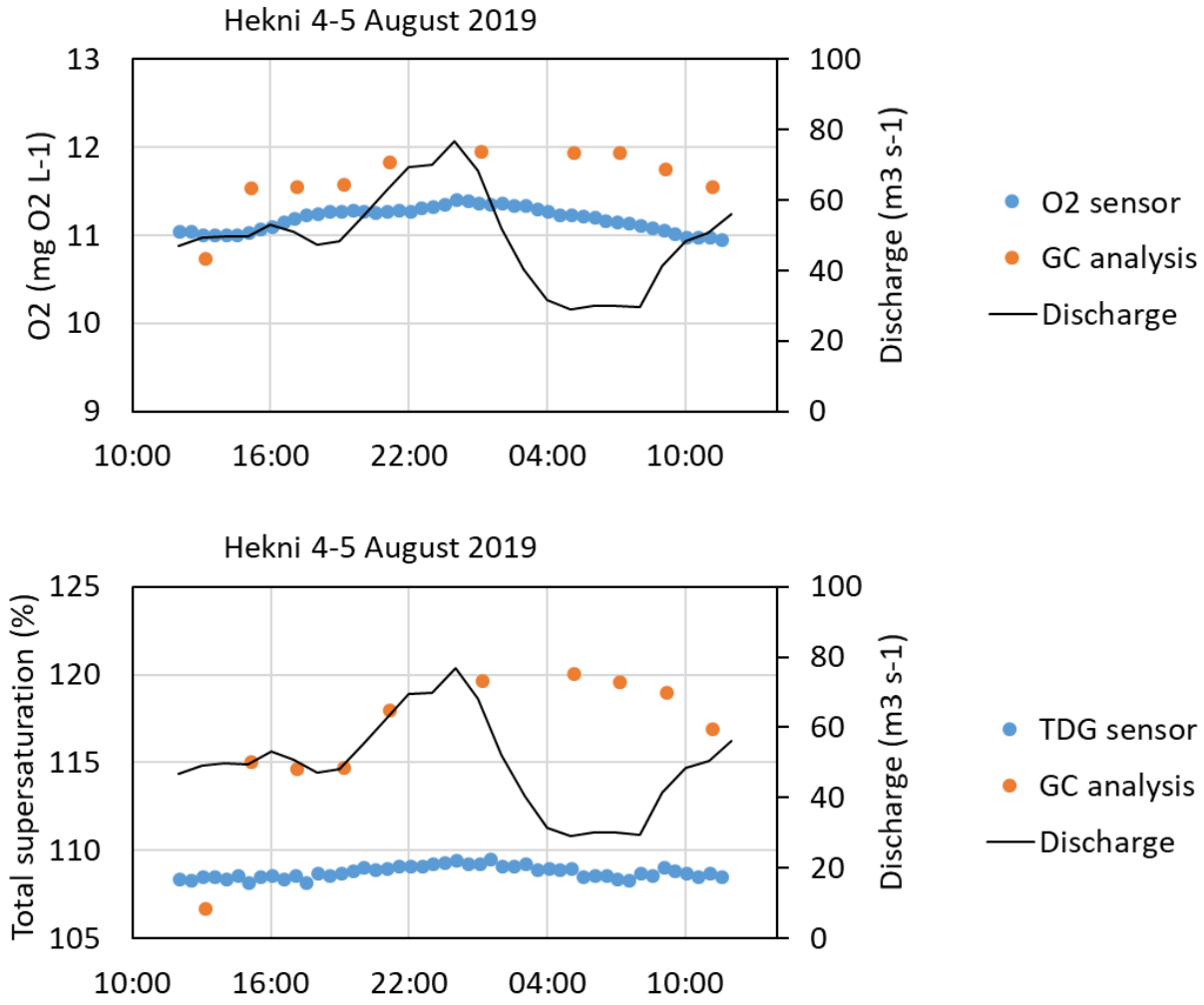

Fig. 5. Most downstream site: Hekni oxygen concentration (upper panel) and total dissolved gas supersaturation (TDG, lower panel). Comparison of data between sensors and determination by gas chromatography (GC). Discharge at Hekni.

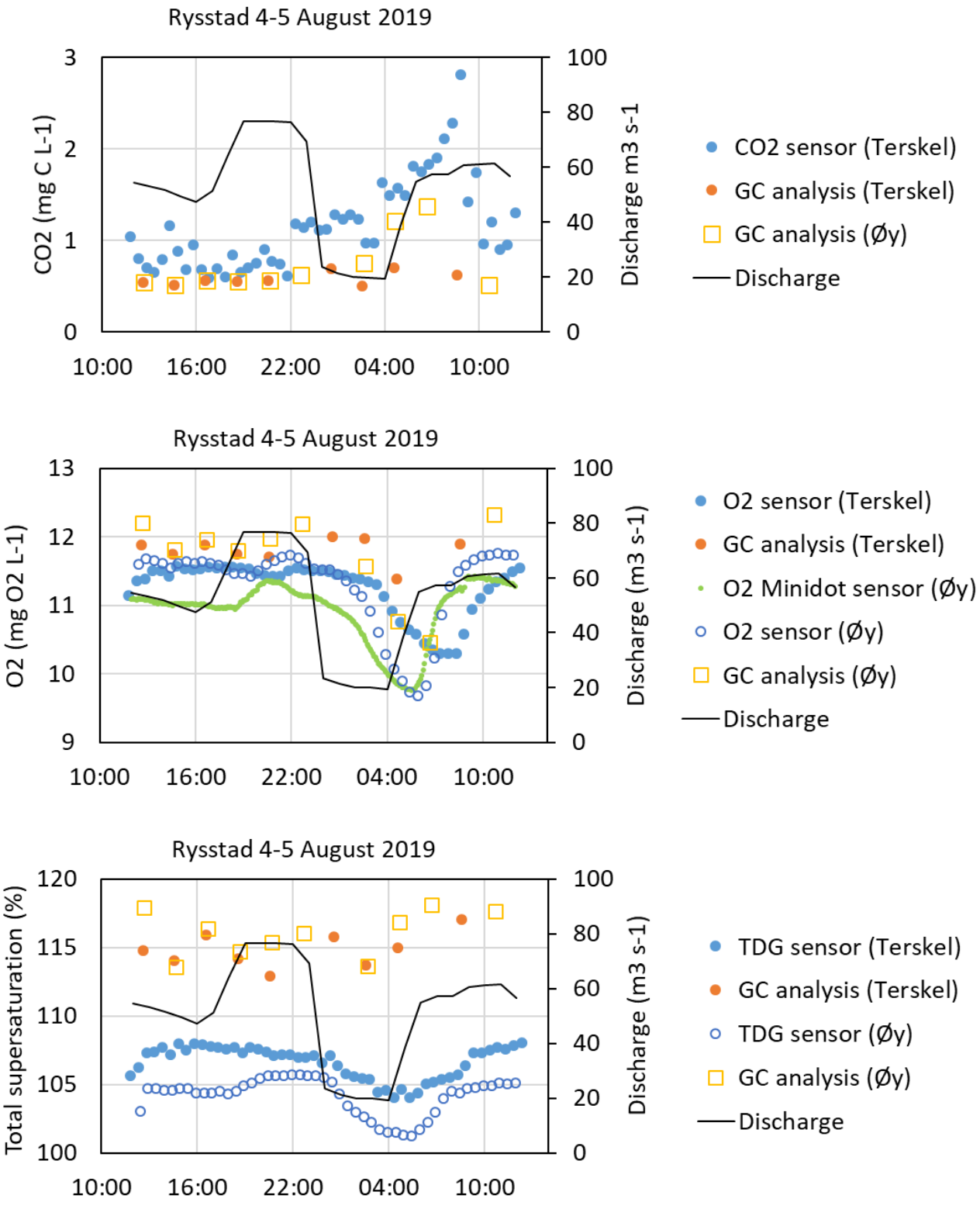

Fig. 6. Bottom station of top section: Rysstad carbon dioxide (upper panel), oxygen (middle panel) and total dissolved gas supersaturation (lower panel). Comparison of data between sensors and determination by gas chromatography (GC). Discharge at Brokke.

3.2 Diel change in dissolved oxygen

Within areas of massive plant growth, we expect O_2 (and CO_2) to change during the day and night (i.e. diel changes) due to the use of CO_2 and production of O_2 by photosynthesis during the daylight hours. This corresponds to our findings, where the largest diel changes in oxygen were observed in the middle and downstream end of the Rysstad basin (middle section with abundant *J. bulbosus* stands) with diel changes of up to 15 % (**Fig. 7**). This is likely due to the combined effects of plant photosynthesis from the mass development of *J. bulbosus* in the middle section (Rysstad to Straume) and lower gas exchange rate than in the upper section (which is a shallower, fast flowing section between Brokke and Rysstad).

3.3 Role of photosynthesis for gas supersaturation

To see the effects of aquatic plant photosynthesis on dissolved oxygen saturation, we used the ratio of oxygen to argon (O_2:Ar). More specifically, this was expressed by the ratio of the excess partial pressure of oxygen relative to argon (EpO_2:EpAr). Diel changes in dissolved oxygen saturation was strongest at Straume (downstream end of the middle section, i.e. the Rysstad basin) with an excess partial pressure of 1.10-1.11 (i.e. 110-111 % dissolved O_2 saturation) from 17:00 to 23:00. This can be seen as the changes through the day of the green dots in **Fig. 8**. As a comparison, there is no such diel change at the Brokke outlet, where there are few plants (black dots in **Fig. 8**). The diel changes in O_2 were mirrored by diel changes in CO_2 (blue dots in **Fig. 9**), as expected for a system with low reaeration, although diel changes in CO_2 due to changes in discharge cannot be completely ruled out (**Fig. 9**).

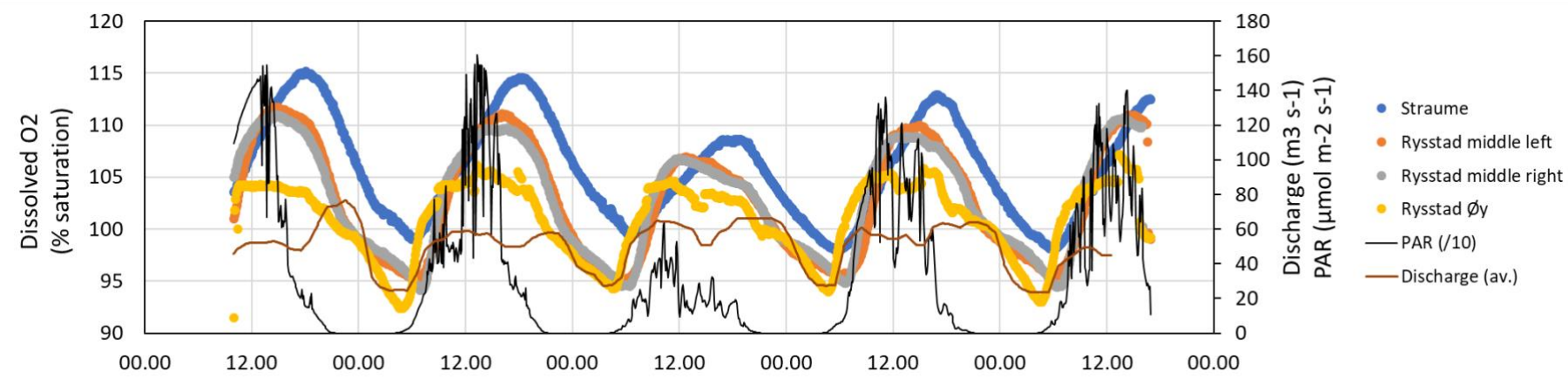

Fig. 7. Diel change in dissolved oxygen saturation at four NIVA monitoring stations in the middle section (from Rysstad to Straume), with changes in discharge and photosynthetic active radiation (PAR), 4th to 8th of August 2019. Discharge was averaged from Brokke and Hekni.

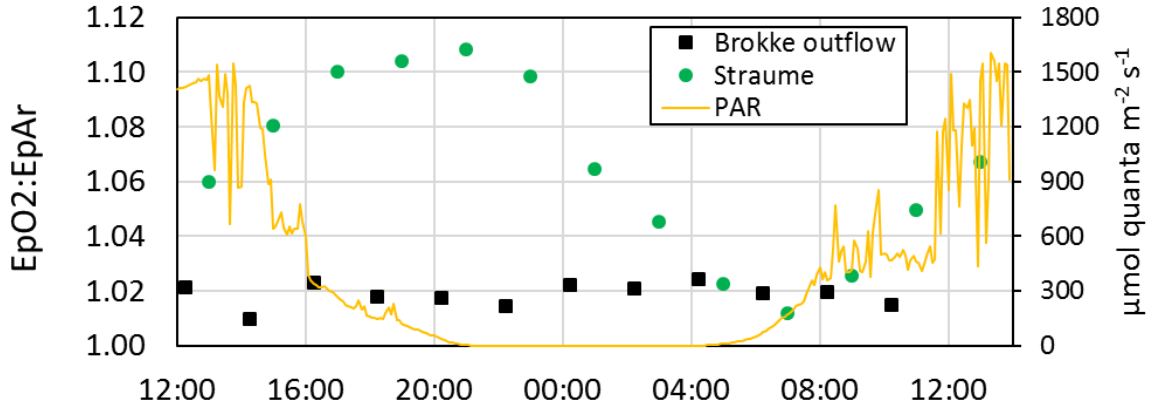

Fig. 8. Excess partial pressure (×100 to get % saturation) of dissolved oxygen standardised by dissolved argon in the outflow of Brokke power plant and at the downstream end of Rysstad basin (average of the two Straume stations). The diel changes at Straume are due to plant photosynthesis, increasing during daylight and decreasing during night-time (PAR, µmol quanta m^{-2} s^{-1}).

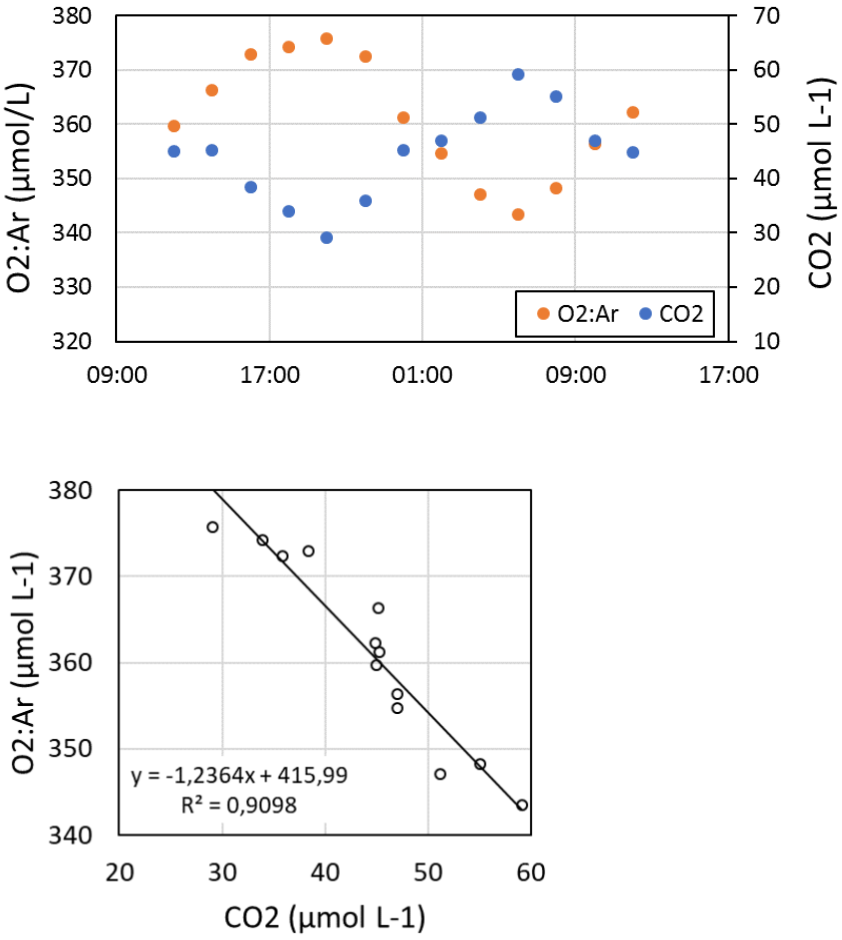

Fig. 9. Concurrent diel changes in O_2 and CO_2 at Straume (downstream end of Rysstad basin). The O_2 concentrations were standardised against Ar, O_2:Ar per sample × average Ar across all samples. There is a nearly one to one diel change in O_2 and CO_2, as can be seen in the bottom graph.

4 Conclusion

To what extent does O_2 produced by aquatic plants during photosynthesis increase the TDG supersaturation downstream of the Brokke Hydropower plant, which in turn may cause harmful effects on fish?

Dissolved O_2 represented about 33-41 % of the total dissolved gases (on August 5th 2019 at Straume), of which up to 10 % were from plant photosynthesis. Thus, plant photosynthesis contributed an additional 3.3-4.1 % oxygen supersaturation at Straume, and 3.0-3.8 % TDG supersaturation after removing the effect of CO_2 uptake by photosynthesis and differential in gas transfer between O_2 and CO_2 at the water–atmosphere interface (see introduction). **Plant photosynthesis could therefore raise total dissolved gas supersaturation by 3.8 %.**

To what extent does CO_2 supersaturation cause increased photosynthesis of aquatic plants, which in turn may cause increased levels of supersaturation and harmful effects on fish?

Assuming 28 % increase in plant photosynthesis, diel change in dissolved oxygen may reach 13 % of dissolved O_2 gas saturation (on the 5th August 2019 at Straume), and plant photosynthesis would thus contribute an additional 4.2-5.2 % oxygen supersaturation at Straume, and 3.9-4.8 % TDG supersaturation after removing the effect of CO_2 uptake by photosynthesis and differential in gas transfer between O_2 and CO_2 at the water–atmosphere interface (see introduction). **Hence an increase of 28 % in CO_2 concentrations could raise total dissolved gas supersaturation due to photosynthesis by another 1 %.**

In sum, outgrowths of *J. bulbosus* may add a maximum of about 5 % to the TDG supersaturation in later afternoon-early evening (4-hour period). This is increasing the risk of bubble formation and expected risks of acute mortality for fish if the added gas saturation causes the TDG supersaturation to increase to levels above a species' tolerance. As an example, the tolerance is 110 % TDG for Atlantic salmon in surface waters, although animals can better tolerate O_2 than N_2 supersaturation.

Since TDG is reduced by about 10 % per meter water depth, fish can potentially escape harmful supersaturation by moving deeper when possible. For example, Atlantic salmon at 3 m water depth may experience acute mortality if the added oxygen causes an increase in TDG saturation on the water surface from 140 to 144 %. This is because the TDG supersaturation at 3 m depth would increase from 110 % to 114 %. It is also important to note that the timing of the dissolved oxygen saturation peak corresponds to the timing of surface feeding by salmonids (personal observation), thus further research linking individual fish behaviour to total gas supersaturation and the role of photosynthesis is needed.

5 References

Binzer T., Sand-Jensen K. & Middelboe A.-L. (2006) Community photosynthesis of aquatic macrophytes. *Limnology and Oceanography,* **51,** 2722-2733.

Blackmann F.F. & Smith A.M. (1911) Experimental researches on vegetable assimilation and respiration. IX. On assimilation in submerged water plants and its relation to the concentration of carbon dioxide and other factors. *Proceedings of the Royal Society of London Series B, Biological Sciences,* **83,** 389-412.

Carroll J.J., Slupsky J.D. & Mather A.E. (1991) The solubility of carbon dioxide in water at low pressure. *Journal of Physical and Chemical Reference Data,* **20,** 1201-1209.

Craig H. & Hayward T. (1987) Oxygen supersaturation in the ocean - Biological versus physical contributions. *Science,* **235,** 199-202.

Emerson S. (1975) Chemically enhanced CO2 gas exchange in a eutrophic lake: A general model. *Limnology and Oceanography,* **20,** 743-753.

Fickeisen D.H., Schneider M.J. & Montgomery J.C. (1975) A comparative evaluation of the Weiss saturometer. *Transactions of the American Fisheries Society,* **104,** 816-820.

Hamme R.C. & Emerson S.R. (2004) The solubility of neon, nitrogen and argon in distilled water and seawater. *Deep-Sea Research Part I-Oceanographic Research Papers,* **51,** 1517-1528.

Johnson E.L., Clabough T.S., Caudill C.C., Keefer M.L., Peery C.A. & Richmond M.C. (2010) Migration depths of adult steelhead Oncorhynchus mykiss in relation to dissolved gas supersaturation in a regulated river system. *Journal of Fish Biology,* **76,** 1520-1528.

Millero F.J., Huang F. & Laferiere A.L. (2002) Solubility of oxygen in the major sea salts as a function of concentration and temperature. *Marine Chemistry,* **78,** 217-230.

Moe T.F. & Demars B.O.L. (2017) Årsrapport krypsivovervåking 2017. Vol. L.NR. 7202-2017. NIVA, Oslo.

Pulg U., Isaksen T.E., Velle G., Stranzl S., Espedal E.O., Vollset K.W., Bye-Ingebrigtsen E. & Barlaup B.T. (2018) Gassovermetning i vassdrag – en kunnskapsoppsummering. Uni Research Miljø LFI rapport 312. ISSN 1892-8889, Uni Research Bergen.

Pulg U., Stranzl S., Vollset K.W., Barlaup B.T., Olsen E., Skår B. & Velle G. (2016a) Gassmetning i Otra nedenfor Brokke kraftverk. Laboratorium for ferskvannsøkologi og innlandsfiske (LFI), UNI Research Miljø, Bergen.

Pulg U., Vollset K.W., Velle G. & Stranzl S. (2016b) First observations of saturopeaking: Characteristics and implications. *Science of the Total Environment,* **573,** 1615-1621.

Roelofs J.G.M., Brandrud T.E. & Smolders A.J.P. (1994) Massive expansion of *Juncus bulbosus* L. after liming of acidified SW Norwegian lakes. *Aquatic Botany,* **48,** 187-202.

Roelofs J.G.M., Schuurkes J.a.a.R. & Smits A.J.M. (1984) Impact of acidification and eutrophication on macrophyte communities in soft waters. II. Experimental studies. *Aquatic Botany,* **18,** 389-411.

Sand-Jensen K. (1987) Environmental control of bicarbonate use among freshwater and marine macrophytes. In: *Plant Life in Aquatic and Amphibious Habitats.* (Ed R.M.M. Crawford), pp. 99-112. Blackwell Scientific Publications, Oxford.

Sculthorpe C.D. (1967) *The biology of aquatic vascular plants,* Edward Arnold Publishers Ltd, London.

Stenberg S.K., Velle G., Pulg U. & Skoglund H. (2020) Acute effects of gas supersaturation on Atlantic salmon smolt in two Norwegian rivers. *Hydrobiologia***, https://doi.org/10.1007/s10750-10020-04439-z**.

Stumm W. & Morgan J.J. (1981) *Aquatic Chemistry. An introduction emphasizing chemical equilibria in natural waters,* Wiley Interscience, New York.

Svedang M.U. (1992) Carbon dioxide as a factor regulating the growth dynamics of Juncus bulbosus. *Aquatic Botany,* **42,** 231-240.

Velle G., Halvorsen G.A., Pulg U. & Olsen E. (2017) Påvirkning fra gassovermetning på bunndyr i Otra nedstrøms Brokke. p. 26. Uni Research Miljø LFI rapport 283, Bergen.

Weiss R.F. (1970) The solubility of nitrogen, oxygen and argon in water and seawater. *Deep-Sea Research,* **17,** 721-735.

Weiss R.F. & Price B.A. (1980) Nitrous oxide solubility in water and seawater. *Marine Chemistry,* **8,** 347-359.

Weitkamp D.E. & Katz M. (1980) A review of dissolved gas supersaturation literature. *Transactions of the American Fisheries Society,* **109,** 659-702.

Yamamoto S., Alcauskas J.B. & Crozier T.E. (1976) Solubility of methane in distilled water and seawater. *Journal of Chemical and Engineering Data,* **21,** 78-80.

Yang H., Andersen T., Dorsch P., Tominaga K., Thrane J.E. & Hessen D.O. (2015) Greenhouse gas metabolism in Nordic boreal lakes. *Biogeochemistry,* **126,** 211-225.

Appendix A.

Fig. S1. Gas chromatograph (red circle) in the lab at NMBU, Ås. Photo: Benoît Demars/NIVA.

Fig. S2. Water samples warming up to lab temperature before creation of a helium head space for the gas chromatograph. NMBU, Ås. Photo: Benoît Demars/NIVA.

Appendix B.

Exact time of sampling (hh:mm), water temperature (°C), absolute atmospheric pressure (mbar), photosynthetic active radiation (PAR, µmol quanta m^{-2} s^{-1}). Temperature and atmospheric pressure allow to calculate percentage saturation from dissolved gas concentrations presented in **Appendix C**.

Exact time	Brokke outflow	Brokke upstream	Hekni	Rysstad Øy	Rysstad terskel	Straume left	Straume right
04.08.2019 12:00	12:15	12:20	13:10	12:40	12:35	13:05	13:00
04.08.2019 14:00	14:15	14:20	15:10	14:40	14:35	15:05	15:00
04.08.2019 16:00	16:15	16:20	17:10	16:40	16:35	17:05	17:00
04.08.2019 18:00	18:15	18:20	19:10	18:40	18:35	19:05	19:00
04.08.2019 20:00	20:15	20:20	21:10	20:40	20:35	21:05	21:00
04.08.2019 22:00	22:15	22:20	23:10	22:40	22:35	23:05	23:00
05.08.2019 00:00	00:15	00:20	01:10	00:40	00:35	01:05	01:00
05.08.2019 02:00	02:15	02:20	03:10	02:40	02:35	03:05	03:00
05.08.2019 04:00	04:15	04:20	05:10	04:40	04:35	05:05	05:00
05.08.2019 06:00	06:15	06:20	07:10	06:40	06:35	07:05	07:00
05.08.2019 08:00	08:15	08:20	09:10	08:40	08:35	09:05	09:00
05.08.2019 10:00	10:15	10:20	11:10	10:40	10:35	11:05	11:00
05.08.2019 12:00	12:15	12:20	13:10	12:40	12:35	13:05	13:00

Temperature	Brokke outflow	Brokke upstream	Hekni	Rysstad Øy	Rysstad terskel	Straume left	Straume right
04.08.2019 12:00	9.3	20.0	11.4	11.0	11.0	11.4	11.4
04.08.2019 14:00	9.3	20.0	11.3	11.3	11.3	12.8	12.8
04.08.2019 16:00	9.6	20.0	11.2	11.2	11.2	13.9	13.9
04.08.2019 18:00	9.5	20.0	11.4	11.3	11.3	14.3	14.3
04.08.2019 20:00	8.2	20.0	12.2	9.7	9.8	14.1	14.1
04.08.2019 22:00	8.5	20.0	13.3	8.7	8.7	13.4	13.4
05.08.2019 00:00	8.5	20.0	13.5	9.0	9.0	12.6	12.6
05.08.2019 02:00	8.5	20.0	13.3	9.1	9.0	11.8	11.8
05.08.2019 04:00	8.5	20.0	13.1	10.6	10.5	11.8	11.8
05.08.2019 06:00	8.5	20.0	12.8	11.7	11.7	11.0	11.1
05.08.2019 08:00	8.4	20.0	12.6	9.9	9.9	10.8	10.8
05.08.2019 10:00	8.6	20.0	12.2	9.9	9.9	10.9	10.8
05.08.2019 12:00	8.9	20.0	11.0	10.3	10.2	11.1	11.1

Pressure	Brokke outflow	Brokke upstream	Hekni	Rysstad Øy	Rysstad terskel	Straume left	Straume right
04.08.2019 12:00	982	982	981	982	982	981	981
04.08.2019 14:00	981	981	980	981	981	980	980
04.08.2019 16:00	980	980	980	980	980	980	980
04.08.2019 18:00	980	980	980	980	980	980	980
04.08.2019 20:00	980	980	980	980	980	980	980
04.08.2019 22:00	980	980	980	980	980	980	980
05.08.2019 00:00	981	981	981	981	981	981	981
05.08.2019 02:00	981	981	981	981	981	981	981
05.08.2019 04:00	981	981	981	981	981	981	981
05.08.2019 06:00	980	980	980	980	980	980	980
05.08.2019 08:00	980	980	980	980	980	980	980
05.08.2019 10:00	980	980	979	979	979	979	979
05.08.2019 12:00	979	979	978	979	979	978	978

PAR	Brokke outflow	Brokke upstream	Hekni	Rysstad Øy	Rysstad terskel	Straume left	Straume right
04.08.2019 12:00	1420	1426	965	1463	1447	1263	1484
04.08.2019 14:00	1422	1332	702	1188	1193	652	642
04.08.2019 16:00	340	330	240	316	329	255	267
04.08.2019 18:00	147	153	110	169	209	117	124
04.08.2019 20:00	37	32	1	13	17	2	3
04.08.2019 22:00	0	0	0	0	0	0	0
05.08.2019 00:00	0	0	0	0	0	0	0
05.08.2019 02:00	0	0	0	0	0	0	0
05.08.2019 04:00	1	1	14	4	3	13	11
05.08.2019 06:00	77	85	196	128	114	179	172
05.08.2019 08:00	357	373	535	516	464	578	414
05.08.2019 10:00	469	489	410	497	525	456	461
05.08.2019 12:00	1179	763	563	1350	1300	1549	1458

Appendix C.

Determination of six dissolved gases (N_2O, CO_2, O_2, N_2, Ar, CH_4) at NMBU by gas chromatography from samples collected at two hourly intervals at seven sites (**Table 1, Fig. 3**). Some bottles were stored too close to the back of the fridge and broke (NA=not available), two samples were likely biased by sampling too close to the shore and walking on soft sediment during the very low flow period (Rysstad Øy at 2:00 and 4:00), two samples were outliers likely for analytical reasons (Hekni 22:00 and Brokke upstream 12:00 on 5 Aug). Outliers are in red and were not discussed in the report.

N_2O nmol L^{-1}	Brokke outflow	Brokke upstream	Hekni	Rysstad Øy	Rysstad terskel	Straume left	Straume right
04.08.2019 12:00	16	12	13	16	16	9	17
04.08.2019 14:00	16	10	15	15	15	17	16
04.08.2019 16:00	17	12	16	16	16	16	17
04.08.2019 18:00	16	12	13	16	15	13	16
04.08.2019 20:00	13	9	13	13	13	13	17
04.08.2019 22:00	13	10	14	14	NA	14	NA
05.08.2019 00:00	15	10	15	NA	14	13	14
05.08.2019 02:00	15	11	NA	16	15	14	15
05.08.2019 04:00	14	NA	14	16	15	13	14
05.08.2019 06:00	15	11	14	17	NA	14	16
05.08.2019 08:00	15	11	13	NA	14	14	NA
05.08.2019 10:00	15	11	14	15	NA	14	16
05.08.2019 12:00	NA	10	NA	NA	NA	15	NA

CO_2 µmol L^{-1}	Brokke outflow	Brokke upstream	Hekni	Rysstad Øy	Rysstad terskel	Straume left	Straume right
04.08.2019 12:00	57	41	43	45	45	49	41
04.08.2019 14:00	62	29	57	42	43	45	45
04.08.2019 16:00	63	42	55	47	47	42	35
04.08.2019 18:00	62	42	46	46	46	33	35
04.08.2019 20:00	53	39	43	46	47	30	28
04.08.2019 22:00	46	44	37	51	NA	36	NA
05.08.2019 00:00	54	46	36	NA	58	41	50
05.08.2019 02:00	54	50	NA	62	42	46	48
05.08.2019 04:00	55	NA	39	101	58	46	56
05.08.2019 06:00	54	50	42	114	NA	55	63
05.08.2019 08:00	56	47	47	NA	51	55	NA
05.08.2019 10:00	54	38	48	43	NA	51	43
05.08.2019 12:00	NA	36	NA	NA	NA	45	NA

O_2 µmol L^{-1}	Brokke outflow	Brokke upstream	Hekni	Rysstad Øy	Rysstad terskel	Straume left	Straume right
04.08.2019 12:00	374	303	335	381	371	353	371
04.08.2019 14:00	378	255	360	369	367	358	373
04.08.2019 16:00	375	304	361	374	371	356	377
04.08.2019 18:00	376	304	362	369	367	360	368
04.08.2019 20:00	385	297	369	374	366	358	374
04.08.2019 22:00	384	300	494	381	NA	361	NA
05.08.2019 00:00	385	297	373	NA	375	349	368
05.08.2019 02:00	389	296	NA	362	374	369	356
05.08.2019 04:00	387	NA	373	337	356	351	359
05.08.2019 06:00	395	300	373	327	NA	351	353
05.08.2019 08:00	389	303	367	NA	372	350	NA
05.08.2019 10:00	383	304	361	385	NA	354	375
05.08.2019 12:00	NA	367	NA	NA	NA	359	NA

N_2 µmol L^{-1}	Brokke outflow	Brokke upstream	Hekni	Rysstad Øy	Rysstad terskel	Straume left	Straume right
04.08.2019 12:00	752	553	651	721	701	668	693
04.08.2019 14:00	754	475	695	686	692	660	676
04.08.2019 16:00	751	562	695	706	704	647	676
04.08.2019 18:00	747	560	698	693	690	654	653
04.08.2019 20:00	779	563	705	736	717	646	680
04.08.2019 22:00	781	575	1169	759	NA	656	NA
05.08.2019 00:00	781	579	693	NA	748	654	701
05.08.2019 02:00	787	577	NA	732	743	744	691
05.08.2019 04:00	788	NA	704	713	720	690	713
05.08.2019 06:00	799	584	703	692	NA	697	709
05.08.2019 08:00	787	582	704	NA	745	690	NA
05.08.2019 10:00	775	566	698	746	NA	681	722
05.08.2019 12:00	NA	785	NA	NA	NA	683	NA

Ar µmol L^{-1}	Brokke outflow	Brokke upstream	Hekni	Rysstad Øy	Rysstad terskel	Straume left	Straume right
04.08.2019 12:00	17.9	13.7	15.9	17.6	17.2	16.3	17.0
04.08.2019 14:00	18.3	11.6	17.0	17.0	16.9	16.2	16.8
04.08.2019 16:00	17.9	13.8	16.8	17.2	17.1	15.8	16.7
04.08.2019 18:00	18.0	13.8	16.9	16.9	16.8	16.0	16.3
04.08.2019 20:00	18.4	13.7	16.9	17.5	17.1	15.8	16.5
04.08.2019 22:00	18.5	14.1	21.7	18.2	NA	16.0	NA
05.08.2019 00:00	18.4	14.0	16.8	NA	18.0	15.9	17.0
05.08.2019 02:00	18.6	14.0	NA	17.6	17.7	17.1	16.8
05.08.2019 04:00	18.4	NA	16.9	17.1	17.2	16.6	17.3
05.08.2019 06:00	18.9	14.2	17.0	16.6	NA	16.8	17.1
05.08.2019 08:00	18.6	13.9	16.9	NA	17.6	16.6	NA
05.08.2019 10:00	18.4	13.7	16.9	17.7	NA	16.4	17.4
05.08.2019 12:00	NA	16.2	NA	NA	NA	16.4	NA

CH_4 µmol L^{-1}	Brokke outflow	Brokke upstream	Hekni	Rysstad Øy	Rysstad terskel	Straume left	Straume right
04.08.2019 12:00	0.031	0.104	0.479	0.108	0.187	0.921	0.854
04.08.2019 14:00	0.048	0.082	0.417	0.096	0.144	0.957	0.885
04.08.2019 16:00	0.052	0.128	0.400	0.117	0.166	0.865	1.119
04.08.2019 18:00	0.052	0.138	0.512	0.127	0.186	1.004	0.954
04.08.2019 20:00	0.031	0.141	0.571	0.092	0.158	1.043	0.901
04.08.2019 22:00	0.050	0.139	0.553	0.075	NA	1.049	NA
05.08.2019 00:00	0.053	0.130	0.495	NA	0.107	0.971	0.872
05.08.2019 02:00	0.050	0.137	NA	0.227	0.162	0.857	0.770
05.08.2019 04:00	0.052	NA	0.500	1.056	0.364	0.658	0.698
05.08.2019 06:00	0.041	0.140	0.551	1.221	NA	0.714	0.739
05.08.2019 08:00	0.040	0.140	0.534	NA	0.187	0.770	NA
05.08.2019 10:00	0.048	0.127	0.520	0.094	NA	0.955	0.854
05.08.2019 12:00	NA	0.119	NA	NA	NA	0.857	NA

TDG %	Brokke outflow	Brokke upstream	Hekni	Rysstad Øy	Rysstad terskel	Straume left	Straume right
04.08.2019 12:00	117	111	107	118	115	111	115
04.08.2019 14:00	118	94	115	114	114	114	117
04.08.2019 16:00	118	112	115	116	116	114	119
04.08.2019 18:00	118	112	115	115	114	116	117
04.08.2019 20:00	117	111	118	115	113	114	119
04.08.2019 22:00	118	114	183	116	NA	114	NA
05.08.2019 00:00	118	114	120	NA	116	111	119
05.08.2019 02:00	119	114	NA	114	114	121	115
05.08.2019 04:00	119	NA	120	117	115	114	118
05.08.2019 06:00	121	116	120	118	NA	113	116
05.08.2019 08:00	119	115	119	NA	117	112	NA
05.08.2019 10:00	118	112	117	118	NA	111	117
05.08.2019 12:00	NA	147	NA	NA	NA	112	NA

NIVA: Norway´s leading centre of competence in aquatic environmentes

The Norwegian Institute for Water Research (NIVA) is Norway's leading institute for fundamental and applied research on marine and freshwaters. Our research comprises a wide array of environmental, climatic and resource-related fields. NIVA's world-class expertise is multidisciplinary with a broad scientific scope. We combine research, monitoring, evaluation, problem-solving and advisory services at international, national and local levels.

Norwegian Institute for Water Research

Gaustadalléen 21 • NO-0349 Oslo, Norway
Telephone: +47 22 18 51 00
www.niva.no • post@niva.no